Scientific paper

Succinyl Curcumin Conjugated Chitosan Polymer-Prodrug Nanomicelles: A Potential Treatment for Type-II Diabetes in Diabetic Balb/C Mice

Sk Mosiur Rahaman,¹ Gouranga Dutta,² Ranu Biswas,^{1,*} Abimanyu Sugumaran,^{3,*} Mohamed M. Salem,⁴ Mohammed Gamal,^{5,*} Mohamed AbdElrahman⁶ and Mounir M. Salem-Bekhit⁷

- ¹ Department of Pharmaceutical Technology, Jadavpur University, Kolkata 700032, West Bengal, India;
- ² Department of Pharmaceutics, SRM College of Pharmacy, SRM Institute of Science and Technology, Kattankulathur 603203, Tamilnadu, India;
- ³ Department of Pharmaceutical Sciences, Assam University (A Central University), Silchar 788011, Assam, India;
 - ⁴ College of Medicine, Huazhong University of Science and Technology, China;
 - ⁵ Pharmaceutical Analytical Chemistry Department, Faculty of Pharmacy, Beni-Suef University, AlshaheedShehata Ahmad Hegazy St., 62514, Beni-Suef, Egypt;
- ⁶ Clinical Pharmacy Department, College of Pharmacy, Al-Mustaqbal University, Babylon, 51001, Iraq;
- ⁷ Department of Pharmaceutics, College of Pharmacy, King Saud University, PO Box 2457, Riyadh 11451, Saudi Arabia.
- * Corresponding author: E-mail: abimanyu.s@aus.ac.in; rbiswas.pharmacy@jadavpuruniversity.in; mgamalm3000@yahoo.com

Received: 02-05-2024

Abstract

Diabetes mellitus is a chronic metabolic disorder marked by elevated blood sugar levels, leading to organ dysfunction. Curcumin, derived from turmeric, exhibits promise in managing type II diabetes. Amphipathic polymer prodrugs were synthesized by conjugating curcumin with chitosan through succinic anhydride. Nanomicelles, formed via dialysis of amphipathic polymer prodrug, were spherical with an average hydrodynamic size of 57 nm. *In vitro* release studies revealed 97% curcumin release at pH 5 in 7 days. A 21-day experiment on diabetic mice compared nano micelles, standard drugs, and free curcumin's impact on fasting blood glucose. The study showcased gradual, controlled curcumin release from nano micelles, suggesting their potential in type II diabetes treatment.

Keywords: Chitosan, Curcumin, nano micelles, polymer-prodrug, Type-II diabetic

1. Introduction

Diabetes mellitus (DM) is a chronic metabolic disorder marked by persistent high blood glucose levels, termed hyperglycemia. Prolonged hyperglycemia can cause significant harm to the body, impairing function and potentially leading to organ and tissue dysfunction. According to the International Diabetes Federation (IDF) in 2021, approximately 10.5% of adults aged 20 to 79 have diabetes, with nearly half undiagnosed. IDF predicts that by 2045, diabetes prevalence among adults will rise to 1 in 8, affecting around 783 million people, marking a 46% increase from current levels. Type 2 diabetes mellitus predominates among major diabetes categories, encompass-

ing around 90% of global diabetes cases.^{3,4} Insufficiency of insulin production (Type 1 diabetes) or diminished cellular sensitivity to insulin (Type 2 and gestational diabetes) are the causes of prolonged hyperglycemia. Insulin-producing β cells are autoimmunely destroyed in type 1 diabetes; the destruction was previously linked to a T-cell-mediated attack. Nevertheless, the cause encompasses both environmental and genetic components, including viral infections, altered intestinal microbiota, and dietary patterns, as well as HLA alleles.⁵ However, it is hypothesized to be associated with suboptimal dietary patterns characterized by high carbohydrate intake and a sedentary lifestyle. There is a gradual transition from a relative shortfall of insulin and lacking with its sensitivity leads to an absolute deficiency, which eventually requires the injection of exogenous insulin to regulate glucose levels.^{3,6,7} Type 2 Diabetes Mellitus (T2DM) traditionally associated with the elderly, is now increasingly prevalent among children and young individuals. This rise is linked to inadequate dietary intake, sedentary lifestyles, and obesity rates. The phytochemical compounds produce a significant therapeutic response in the treatment of metabolic disorders such as diabetes mellitus due to their low toxicity. Curcumin, (CCMN) a polyphenolic phytochemical derived from the rhizome of the turmeric plant (Curcuma longa), has several medicinal properties (like anti-inflammatory, anti-cancer, antioxidant, wound healing, and anti-diabetic etc).8-10 It has a wide range of potential applications and therapeutic activity. Still, its use is limited due to its very low aqueous solubility, chemical instability, photosensitivity, first-pass metabolism, insufficient tissue distribution, and inadequate absorption, resulting in inadequate bioavailability.11-13 Studies have demonstrated that CCMN regulates lipid metabolism by suppressing key inflammatory transcription factors (MCP-1, IL-6, HbA1c, TNF-α), reducing hepatic lipogenesis, and enhancing lipid mobilization enzyme activity. In animal models of diabetes, curcumin exhibits anti-hyperglycemic and anti-hyperlipidemic effects. Additionally, its antioxidant properties mitigate oxidative stress, a factor in Type 2 Diabetes Mellitus development. Curcumin has anti-inflammatory properties via its ability to reduce the levels of inflammatory factors, as well as through blocking signalling pathways such as NF-κB.^{14,15} Moreover, it plays a crucial function in safeguarding heart health via its ability to mitigate apoptosis and inflammation in individuals with diabetic cardiomyopathy. The cumulative data indicate that curcumin may have therapeutic advantages in managing T2DM and its related problems. 16,17 A variety of approaches, including the encapsulation of CCMN in different lipid nanocarriers or the formation of polymer-prodrug complexes, are intended to address these challenges. Polymer-drug conjugates represent a prevalent and efficacious method for the delivery of hydrophobic drugs. This concept, initially introduced by Ringsdorf et al. in 1975, facilitates controlled drug release, enhances

therapeutic efficacy, reduces adverse effects, and improves patient compliance by increasing drug solubility in aqueous solvents. ^{18,19}

Chitosan (CHT), a biopolymer known for its biocompatibility, biodegradability, and ability to form gel-like structures in acidic conditions, is utilized in drug delivery applications. With its glucosamine unit containing hydroxyl and amine groups, chitosan enables the conjugation of many drugs and other substances. 20 This property can improve the drug's solubility, stability, and toxicity and facilitate the delivery of the drug to specific cells or tissues.^{21–23} In this study, we proposed preparing the polymer prodrug conjugate by chemically binding curcumin and chitosan. The conjugation was done in the presence of succinic anhydride, which could act as a bridge between the chitosan and curcumin. This conjugate was converted to nano micelles in an aqueous environment, which may increase CCMN solubility and stability.^{24,25} The in vitro hemocompatibility and physicochemical characteristics was investigated. The therapeutic potentiality, toxicity, and biochemical parameters of nano micelles was examined in in-vivo diabetic Balb/C mice induced by streptozotocin for 21 days.

2. Experimental

2. 1. Materials

Chitosan (low molecular weight ~ 50000 Da) purchased from Sigma-Aldrich, curcumin, succinic anhydride, dimethyl sulfoxide (DMSO), N, N'dicyclohexylcarbodiimide (DCC), 4-dimethylamino pyridine (DMAP), pyrene, pyridine, mono-tetrazolium salt (MTT) and other compounds were purchased from SRL Chem Pvt. Ltd (Mumbai, India). The blood was purchased from the certified blood bank in Kolkata, India. All the chemicals are used as analytical grades.

2. 2. Synthesis of Succinyl-Curcumin Conjugate (SUC-CCMN)

To synthesize SUC-CCMN, initially, CCMN (0.7368 g, 2 mmoL) and succinic anhydride (0.2001 g, 2 mmoL) were dissolved in 30 mL benzene and then added 2mL pyridine consequently refluxed for 36 h at 80 °C. After removal of the solvent under low pressure and lower temperature, the residue was purified by column chromatography, where hexane-ethyl acetate (95:5) was used as the mobile phase and silica gel as a stationary phase to get the final product SUC-CCMN (Yield = 0.32 g, 68.31%).²⁶

2. 3. Synthesis of CHT-di(SUC-CCMN) Conjugates

To synthesize CHT-di(SUC-CCMN) conjugate, initially, in 20 mL DMSO carbohydrate polymer CHT

(1.52 gm, 1 mmoL) and SUC-CCMN (0.93 mg, 2 mmoL) were dissolved at room temperature. After both compounds were dissolved entirely, DCC (412 mg, 2 mmoL) and DMAP (116 mg, 1 mmoL) were added to the mixture while stirring continuously. This reaction was carried out in the dark at room temperature for 24 h. Following the completion of the reaction, the product was filtered to precipitate the CHT-di(SUC-CCMN) conjugate. The filtrate was added into a 50 mL solution containing a 1:1 (v/v) ratio of ethanol and ethyl ether to precipitate CHT-di(SUC-CCMN) conjugate. Figure 1 depicts the schematic processes for CHT-di(SUC-CCMN) synthesis.

2. 4. Preparation of CHT-di(SUC-CCMN) Conjugates Micelles

For the preparation of CHT-di(SUC-CCMN) conjugated micelles (CDSCM), 1 mg/mL CHT-di(SUC-CCMN) was prepared with DMSO by proper mixing. Then CHT-di(SUC-CCMN) mixture was taken into a dialysis bag (Mol.Wt 12 kDa), placed into double distilled water for 24 h, and replaced in 4 h intervals. The solvent remained in the reaction process, and other components were eliminated through dialysis. After completion of dialysis, it was passed through a filter of 0.45 μm pore size to avoid the large particles, then lyophilized the product. The final micelles were stored in a cool and dry place for further use. 27 The yield of CDSCM was about $81\pm6\%$.

2. 4. Physicochemical Characterizations of CDSCM

2. 4. 1. Characterizations of CDSCM

The structure of synthesized CHT-di(SUC-CCMN) was confirmed by different instrumental analyses, like an FTIR spectrophotometer (Shimadzu Corp No. 01988) with a spectral range of 4000 cm⁻¹ to 400 cm⁻¹. ¹H-NMR (Bruker-500 MHz spectrometer) spectral analysis was done with the solvent DMSO-d6 and a UV-vis spectrophotometer (Shimadzu, Japan) over 200-700 nm. To know the morphology, hydrodynamic size, and zeta potential of the CDSCM, a zeta seizer (Nano-ZS 90, Malvern Instrument, UK), field emission scanning electron microscope; FEI, Quanta 200 (FE-SEM). To make the SEM sample, 1 mg/mL of lyophilized CDSCM powder was mixed with 1 mL of double distilled water. Then, the dispersion was placed on an aluminum sheet to make the thin film. The air-dried film was then coated with gold and evaluated under the SEM. A high-resolution transmission electron microscope (HR-TEM) (JEOL Japan, JEM-2100 Plus) was used, and TEM samples were prepared by placing a 0.001 mg/mL drop of CDSCM dispersion on the carbon-coated copper grid.

2. 4. 3. Critical Micelle Concentration (CMC) Determination

To determine the CMC of CHT-di(SUC-CCMN), different concentrations of CHT-di(SUC-CCMN) solutions ranging from 0.004 mg/mL to 2.5 mg/mL were vortexed with diluted fluorescent probe pyrene (used as fluorescent dye) solution. The CHT-di(SUC-CCMN) mixture was left overnight to record fluorescence using a fluorescence spectrophotometer at 390 nm emission (Infinite M200, TECAN).²⁸

2. 5. Drug Loading Capacity

A specified high concentration of CCMN solution was prepared, and various concentrations of CCMN solution were prepared using the serial dilution procedure using DMSO as a solvent. The absorption was measured at 435 nm, and a standard curve was prepared. Absorption was measured after preparing a known concentration (1mg/mL) of CHT-di(SUC-CCMN) conjugate micelle (CDSCM) in DMSO solvent. The quantity of CCMN in the CHT-di(SUC-CCMN) conjugate micelle was determined using the standard line (equation). The following equation was used to compute the CCMN loading capacity of the CHT-di(SUC-CCMN) conjugate in micelles:

$$\frac{\text{CCMN loading capacity } \left(\frac{w}{w}\%\right) =}{\frac{\text{Ammount of CCMN}}{\text{Ammount of CCMN released from CDSCM}}} \times 100} \tag{1}$$

2. 6. Stability of free CCMN and CDSCM in Physiological Conditions

The stability of the compound in different pH is different. The stability of free CCMN and CDSCM were analyzed in PBS buffer pH 7.4 for a specific incubation period at 37 °C, taken absorption by UV–vis spectrophotometer at 427 nm. The change of absorbance in the physiological condition of both compounds was noted and plotted graphically.²⁹

2. 7. CCMN Release Study from CDSCM

In CDSCM, CCMN is conjugated with CHT through pH-sensitive succinyl ester bonds. The cumulative releases of CCMN from CDSCM were measured in PBS buffer pH 5.0 and 7.4. A fixed quantity of CDSCM (10 mg) was dispersed in each 10mL of PBS buffer pH 5.0 and 7.4 solutions. All those solutions were taken into two separate dialysis bags and transferred into 90 mL respective buffer solution containing beakers. Those were incubated at 37 °C for 7 days with moderate shaking. During the incubation period, with an increasing time interval, 2 mL of the sample was withdrawn from each beaker and replaced with the respective buffer.³⁰ A UV-vis spectrophotometer analyzed the concentration of CCMN at 427 nm.

2. 8. Blood Compatibility

A hemolysis study monitored the hemocompatibility of CDSCMs using a blood sample obtained from a local blood bank. RBCs were separated from the blood sample by centrifugation at 2000 rpm for 5 min. The collected RBCs were washed three times in PBS buffer. The stock RBC solution was made by combining 100 µL of washed RBC with 10 mL of PBS (pH 7.4) buffer. To determine the hemoglobin release from RBC by CDSCM, 100 µL of stock RBC solutions were subjected to 100 µL different concentrations of CDSCM ranging from 0.5 to 2 mg/mL for 30 min at 37 °C. Then, all those solutions were centrifuged separately at 1500 rpm for 5 min, and the supernatant was taken for UV-visible absorbance at 541 nm. 31,32 PBS buffer pH 7.4 solution was utilized as a negative control, and distilled water as a positive control. The hemolysis percentage (Hp%) of CD-SCM will be determined using the equation shown below:

$$Hp\% = \frac{As - An}{Ap - An} \times 100 \tag{2}$$

Where A_S = absorbance of the sample, the absorbance of the PBS buffer = A_n , and absorbance of distilled water = A_p . All the readings were taken in triplicate.

2. 9. *In-vivo* Experimental Protocol

2. 9. 1. Experimental Animals

For the *in vivo* antidiabetic activity study, male Balb/C mice weighing about 25–30 g were obtained from Chakraborty Enterprises (North 24 Parganas PIN-743312 West Bengal), registered breeders.^{33,34} Before the start of experiments, they were kept for seven days to adjust standard laboratory conditions with a standard diet according to protocols. This experiment followed the guidelines of the "Institutional Animal Ethics Committee (Registration number: 1805/GO/Re/S/15/ CPCSEA)", Jadavpur University, India (Approval of project proposal No: JU/IAEC-22/30), throughout the study, followed the National Institute of Health (NIH) recommendations.

2. 9. 2. Experiment Design of *In vivo* Study

A total of 30 Animals were taken and equally divided into five groups. Group I: Non-diabetic control animals (NDC) received a high fat-containing regular diet. Group II: Diabetic control (DC) received a high fat-containing regular diet with a single dose of diabetic inducer. Group III: Diabetic control free CCMN (DC-FCUR) received a high fat-containing regular diet with a single dose of diabetic inducer and treated orally with free CCMN at 100 mg/kg body weight for 21 days. Group IV: Diabetic control drug-containing nanoparticle (DC-DCN) received a high fat-containing regular diet with a single dose of diabetic inducer and treated orally with CDSCM equivalent to 100 mg/kg CCMN payload for 21 days. Group V: Diabetic control standard drug (DC-SD),

which received a high fat-containing regular diet with a single dose of diabetic inducer and treated orally with 2mg/kg b.w. glibenclamide for 21 days.

2. 9. 3. Induction of Type-II Diabetes Mellitus

To induce Type-II diabetes mellitus, a single intra¬peritoneal injection of STZ (45 mg/kg to overnight fasting animals) followed by a 110 mg/kg intraperitoneal injection of nicotinamide after 15 min.3 $^{5-37}$ both solution was prepared separately by dissolving in citrate buffer pH 4.5 and saline solution, respectively. Non-diabetic control (Group I) animals were injected with saline instead of STZ. FBG levels of all animals were measured by an accu-check glucometer (Roche Diagnostics) on alternate days. Animals with FBG levels \geq 200 mg/dl for three consecutive days after STZ injection were considered diabetic animals, and animals with blood glucose levels \leq 145 mg/dl were considered non-diabetic animals and were excluded from the experiment.

2. 9. 4. Sampling of Blood to Estimate FBG Level

Blood samples were collected by pricking the tail and then gently milking it with warm water to evaluate the FBG level of each animal. The direction of milking was from the body side to the tail tip to enhance bleeding. One drop of blood was placed on a strip of the accu-check glucometer to take blood glucose levels, and it was done in duplicate to ensure the consistency of glucometer readings.³⁸

2. 9. 5. Measurement of Body Weight

Every four days, the body weight of each animal in each group was measured. The variation in weight was documented. After 21 days, the liver weight of each animal was also recorded.

2. 9. 6. Estimation of Biochemical Parameters Level

For estimating the biochemical parameters, the blood of all animals was collected under mild anesthesia through cardiac puncture on the 21st day of the study. Blood samples were centrifuged for 15 min at 4000 rpm in a cooling centrifuge. Serums were correctly leveled and stored at –80 °C for further analysis. Auto-analyzer (USA) and ELISA kits for estimating the level of a lysosomal enzyme like alkaline phosphatase (ALP) (rAPid Alkaline Phosphatase; Roche), acid phosphatase (ACP) (CS0740, Sigma Aldrich), lipid profile components like HDL, LDL, serum triglycerides (TGL), total serum cholesterol, liver-specific enzymes like serum glutamate oxaloacetic transaminase (SGOT), serum glutamate pyruvic transaminase (SGPT), Hemoglobin A1c (HbA1c) (CS0740, Sigma Aldrich) and serum uric acid.^{38,39}

2. 9. 7. Carbohydrate Metabolizing Enzymes Estimation

To estimate the level of hexokinase (HK), glucose-6-phosphate dehydrogenase (G6PD), and lactate dehydrogenase (LDH) parameters in the pancreas, liver, and kidney, all animals were euthanized with thiopental sodium after 21 days of treatment. Those tissues (0.3 g) were taken separately and homogenized in 3 mL of 0.01M Tris-HCL centrifuged at 10000 rpm for 20 min at 4 °C. Supernatants were treated with the corresponding colorimetric assay kits for HK, G6PD, and LDH.^{39,40}

2. 10. Statistical Analysis

For the statistical analysis, all the readings were taken more than two times, standard deviation (SD) was calculated from obtained data, and the actual value of the readings was represented as mean \pm SD, were it possible. For the statistical processing of obtained results, one-way analysis of variance (ANOVA) with P-value < 0.05 was used to know the groups/category significant changes in another statistical tool, like a student t-test. Different software like Origin Pro 9.0 and GraphPad Prism 6.0 are used for the graphical representation of statistically processed data.

3. Results

The primary objective of our investigation was to synthesize the CHT-CCMN conjugate, which was subsequently synthesized and characterized using various instrumental methods. After confirming the synthesis of the conjugate, it was found that the conjugate was freely soluble in an aqueous and non-aqueous solvent. The tri-molecular conjugated polymer-prodrug, consisting of a hydrophilic polymer and hydrophobic drugs, can enhance aqueous solubility, improve drug targeting, prevent drug resistance, and minimize the toxic effect of the desired drug. 41,42 This study used CHT as a hydrophilic polymer, CCMN as a hydrophobic drug, and succinic anhydride as a bi-molecular pH-sensitive linker. CCMN, when conjugated with CHT via a succinyl ester link, creates an amphiphilic polymer-prodrug known as CHT-di (SUC-CCMN). This prodrug self-assembles into nano micelles when placed in an aqueous media. CHT has several hydroxyl groups that have the capability to form bonds with multiple SUC-CCMN molecules, enabling the transportation of CCMN for drug delivery purposes.

For the formation of CHT-di(SUC-CCMN) prodrug conjugate, CCMN refluxes with succinic anhydride in the presence of pyridine to form SUC-CCMN, which consists of a carboxylic acid group that can further react with a hydroxyl group of CHT to form an ester bond by a condensation reaction in the presence of pyridine, as shown in Figure 1. The FT-IR spectrum of CCMN clearly shows characteristic peaks of phenolic O-H stretching at 3507 cm⁻¹ for aromatic moiety C=C stretching peak at 1625 cm⁻¹, benzene ring stretching vibrations peak at 1596 cm⁻ ¹, for C=O and C=C vibrations peak at 1504 cm⁻¹, for C-H bending vibrations of olefinic (>C=C<) bond peak at 1424 cm⁻¹ and for stretching vibrations of the aromatic C-O bonding peak at 1276 cm⁻¹ could identify CCMN (Figure 2). 43,44 The FT-IR spectrum of SUC-CCMN shows a peak for phenolic O-H stretching at 3505 cm⁻¹, a peak for aryl

Figure 1. The schematic reactions for synthesizing SUC-CCMN and CHT-di(SUC-CCMN) conjugate.

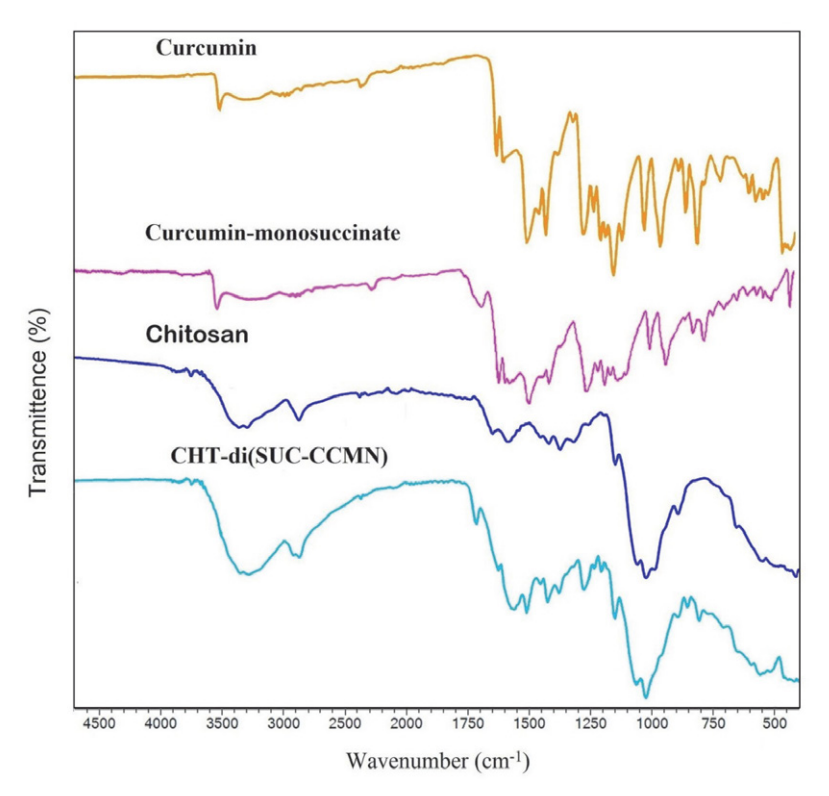


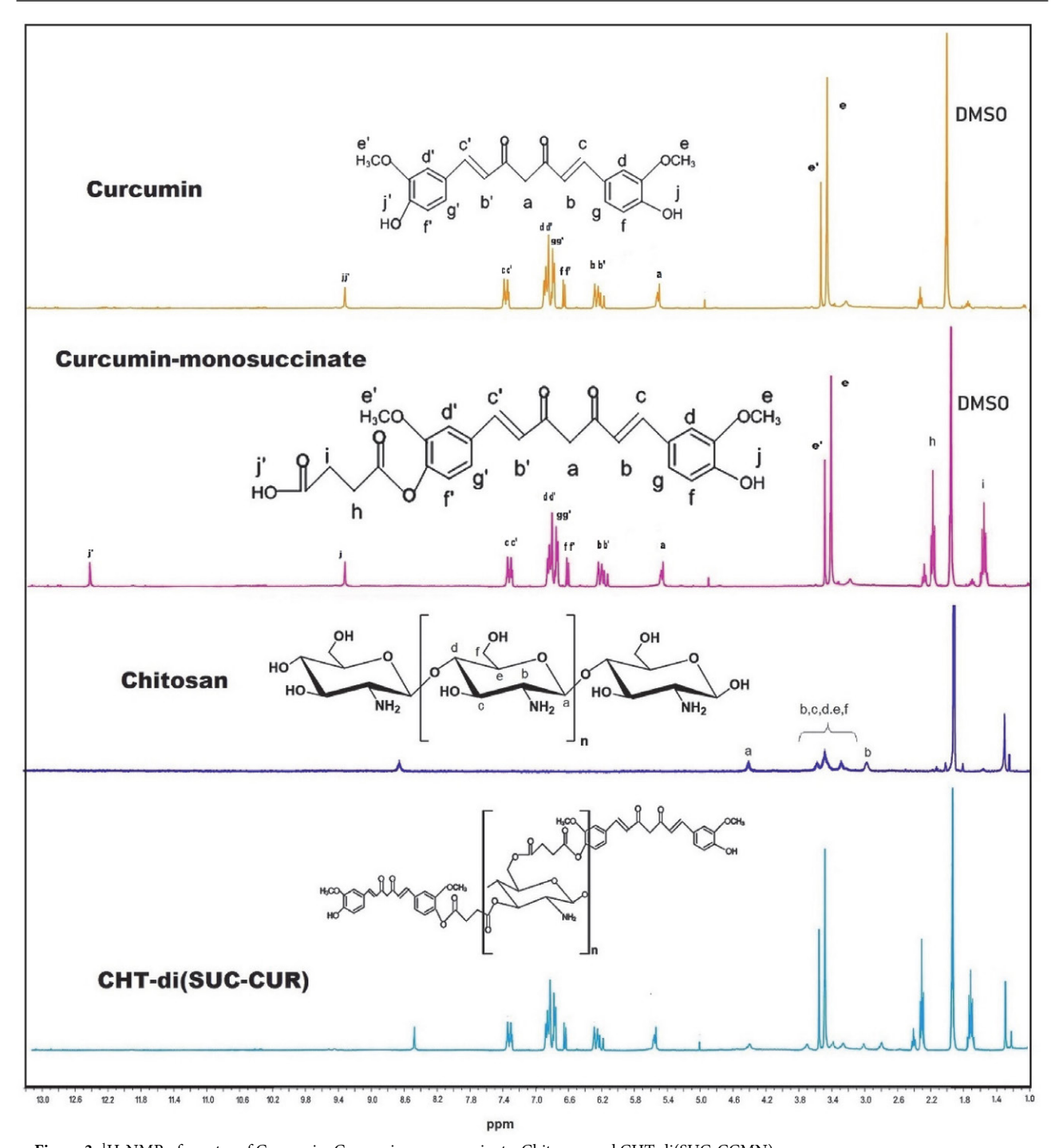
Figure 2: FTIR spectra Curcumin, Curcumin-mono succinate, Chitosan, and CHT-di(SUC-CCMN)

(C-H) stretching at 2942 cm⁻¹, peaks for C=O stretching frequencies of a conjugated succinic acid moiety at 1697cm⁻¹, peak for C=C of CCMN at 1627 cm⁻¹, a peak for stretching frequencies of C=O and C-O (enol) groups of CCMN moiety at 1510cm⁻¹ and 1281 cm⁻¹. The peak at 1028 cm⁻¹ is attributed to the stretching frequencies of C-O-C. The presence of prominent peaks at 3505 cm⁻¹, 1697 cm⁻¹, and 1510 cm⁻¹ corresponding to the -OH, C=O , and C-O bands, respectively, represent the successful conjugation of CCMN to SUC.25 The FT-IR spectrum (Figure 2) of CHT-di(SUC-CCMN) conjugate exhibits a new peak at 1735 cm⁻¹ corresponding to the stretching frequency of the C=O group and a peak at 1510 cm⁻¹ corresponding to the C-O (enol) bands stretching frequencies in addition to peaks exhibited by CHT and SUC-CCMN, those peaks represent the existence of newly formed ester bond between CHT and SUC-CCMN.⁴² The FTIR analysis demonstrates that the procedure begins with the reaction of CCMN and succinic anhydride, which results in the formation of SUC-CCMN with a reactive carboxylic acid group. The FTIR spectrum reveals that this acid group interacts with the hydroxyl group of CHT in the presence of pyridine to form an ester bond, leading to CHT-di(SUC-CCMN) prodrug-polymer synthesis. The enhanced solubility of curcumin in CHT-di(SUC-CCMN) could potentially be attributed to the formation of a tenuous hydrogen bond between the carbonyl group (C=O) in curcumin and the hydroxyl group in chitosan.⁴⁵

To assure the formation of the conjugated structure of CHT-di(SUC-CCMN), CHT, CCMN, and SUC-CCMN

were initially analyzed through ¹H-NMR spectroscopy. In Figure 3, it was observed that protons of CCMN show characteristic peaks between 5.4–9.4 ppm;^{45,46} CHT shows its distinct peaks between 3.0-4.6 ppm for the protons of $\beta(1-4)$ -D-glucosamine units, 47 including peak at 1.3 ppm for the presence of acetylated chitosan impurities; SUC-CCMN shows peak at 2.2 and 2.4 ppm for protons of -CH₂-CH₂- (Succinyl moiety) including the peaks at 9.4 and 12.5 ppm for the -OH proton of CCMN and succinyl moiety respectively in addition to peaks of CCMN. CHTdi(SUC-CCMN) conjugate exhibits its peaks consisting of characteristic peaks of CHT (3.0-4.6 ppm), CCMN (5.4-9.4 ppm), and succinyl (2.0 and 2.5 ppm) moiety excluding the peaks 12.5 ppm of succinyl moiety -OH proton were demonstrated the successful synthesis of desire conjugate. 46,48 Analysis of the CHT-di(SUC-CCMN) conjugate by ¹H-NMR confirmed its successful synthesis. The characteristic peaks of CCMN, CHT, and SUC-CCMN were evident in their respective spectra. Notably, the conjugate's spectrum displayed peaks from all constituents except the -OH proton of the succinyl moiety. This absence and the presence of all other expected peaks strongly supported the construction of the designed conjugate.

To know the presence of CCMN in the CHT-di(SUC-CCMN) conjugate, CCMN and CHT-di(SUC-CCMN) were analyzed by UV-vis and fluorescence spectrometer. Both CCMN and CHT-di(SUC-CCMN) conjugate show peak Uv-absorbance at 427 nm (Figure 4a, 4b), but conjugate shows a broader peak than the CCMN peak. The fluorescence emission spectral peak (the excita-



 $\textbf{Figure 3: } ^1\text{H-NMR of spectra of Curcumin, Curcumin-monosuccinate, Chitosan, and CHT-di(SUC-CCMN)}$

tion wavelength 427 nm) of CCMN and CHT-di(SUC-CCMN) shows at 550 nm and 522 nm, respectively, which help to conclude the formation of the conjugation within CHT and CCMN. 49

The CHT-di(SUC-CCMN) conjugate consists of a free hydroxyl group containing the CHT moiety, which is the hydrophilic part. The CCMN moiety, the hydrophobic domain, jointly helps the amphiphilic to self-assemble into micelles (CDSCM) in an aqueous medium where the hydrophobic part forms the core and the hydrophilic part

remains outside of the micelle. Critical micelle concentration (CMC) signifies a concentration at which the amphiphilic polymeric compound can self-assemble into micelles in the solvent. The CMC of CDSCM was determined by employing the self-quenching agent pyrene as the fluorescence probe in an aqueous medium, and it helps to produce fluorescence for the presence of a lipophilic part of the micellar core. The intensity ratio of pyrene's (I335/I332) peaks depends on the medium's polarity. The fluorescence intensity changed rapidly when pyrene transited

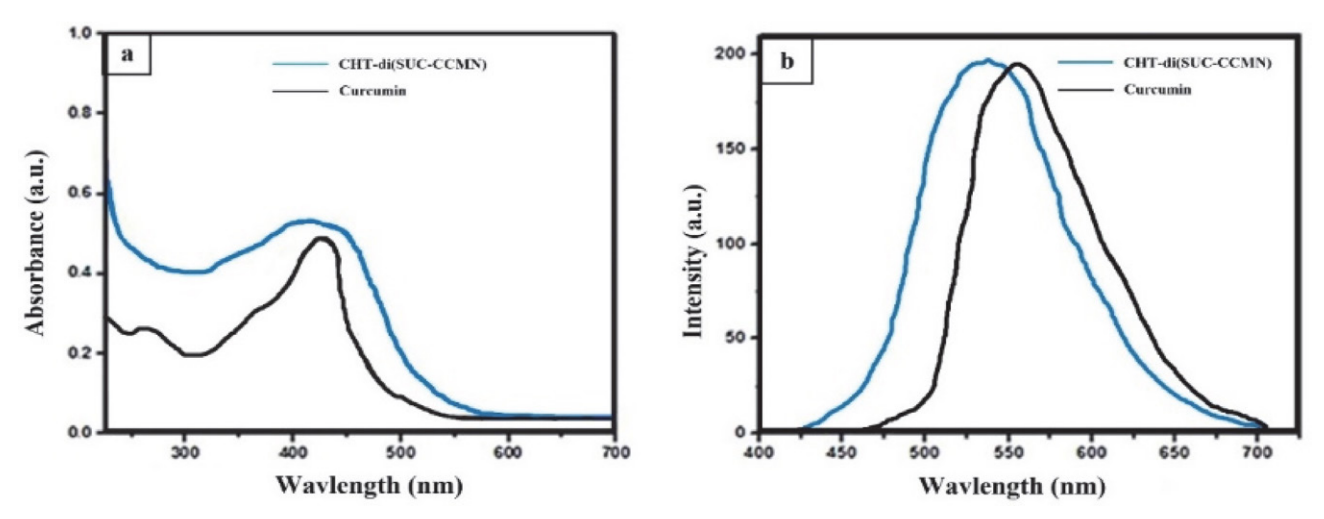


Figure 4: (a) UV-vis and (b) fluorescence spectra of CCMN and CHT-di(SUC-CCMN) conjugate

from hydrophilic media to the lipophilic core of CDSCM. Plotting the logarithm concentration of conjugate vs. intensity ratio constructs two straight lines intersecting at a point called CMC, which was 0.4644 mg/mL (Figure 5A). The lower CMC values signify its stability, prolonging blood circulation and accessibility to the drug's targeting.⁵²

The hydrodynamic particle size and zeta potential of the CDSCM were determined by dynamic light scattering (DLS). The hydrodynamic particle size distribution of CD-SCM is shown in Figure 5C, and zeta potential is shown in Figure 5B. It was observed that micelles were about 57 ± 6 nm in size from and polydispersity index was found to be 0.19 Figure 5C. The zeta potential of CDSCM was meas-

ured to be -34.8 mV, suggesting a significant negative charge. This negative charge is caused by the presence of unbound hydroxyl (-OH) groups in the glucosamine units of the CHT moiety on the surface of CDSCM. This accumulation of hydroxyl groups results in the formation of a highly negatively charged CDSCM surface. This negative change serves to maintain the CDSCM's stability. Higher negative surface charges repel each CDSCM from the other, thereby reducing nano-micelle accumulation. The morphology of CDSCM was also determined through SEM and TEM (Figures 5D, 5E). Figure 5D indicates that CDSCM were roughly spherical and mostly uniform in size. The shape of the particle is distinguishable. For better

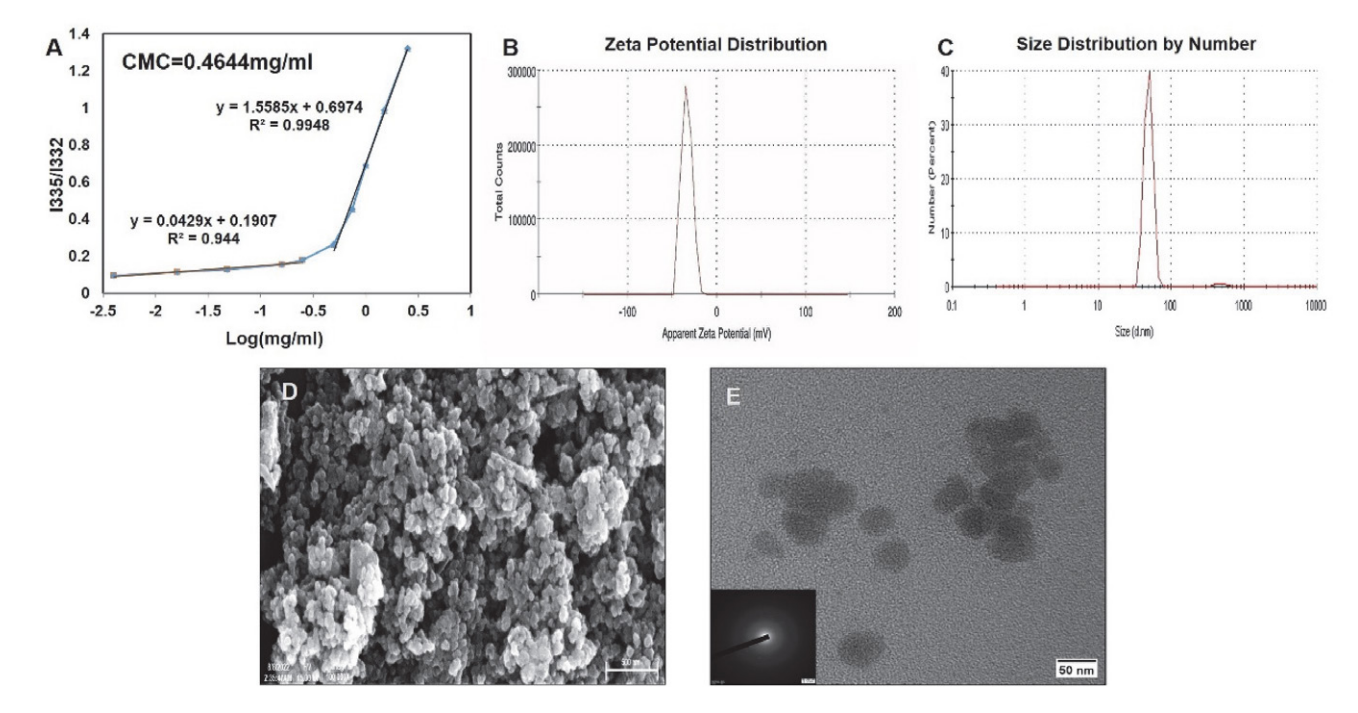


Figure 5. (A) CMC of CHT-di(SUC-CCMN) conjugate; (B) Zeta potential of CDSCM; (C) Particle size distribution of CDSCM; (D) FE-SEM Image of CDSCM; (E) TEM Image of CDSCM

morphological evaluation, another microscopic (TEM) study was done. Figure 5E shows that the CDSCM are spherical in shape and within the size range of 50 nm ±15 nm. The selected area electron diffraction (SAED) pattern in the bottom left corner of the TEM image shows that the CDSCM samples don't have any crystalline particles. Based on the data shown in Figure 5, it is evident that the CDSCM was produced with precision, exhibiting higher zeta potential and smaller particle size. The size of the Nano micelles seen in the TEM analysis was primarily consistent with the hydrodynamic sizes of the Nano micelles determined by DLS analysis. Based on the aforementioned results, it is obvious that the CDSCM has the potential for use in the applications described above.

In physiological pH, the stability of free CCMN and CDSCM was compared. The stability of free CCMN and CCMN in CDSCM was evaluated at pH 7.4. The stability of free and formulated drugs at physiological pH is critical in drug delivery investigations. PBS was used to make a highly concentrated solution of free CCMN and CDSCM (pH 7.4). Absorbance was measured at 427 nm using a UV-vis spectrophotometer at set intervals from both solu-

tions up to a particular period. The percentage of degraded compounds for both compounds was calculated and presented in Figure 6a. It was observed that free CCMN was about to degrade entirely after 8 h, while more than 90% of CCMN in CDSCM was still present at the same time. As a result, conjugated CCMN exist in CDSCM and are much more stable than free CCMN. CCMN micelles developed by conjugation of CCMN with CHT significantly improve CCMN stability (Figure 6a).

The CCMN release pattern from CDSCMs was studied at physiological pH 7.4 and acidic pH 5, as shown in Figure 6b. It was observed that 97% of CCMN was released from CDSCM within 7 days in an acidic (pH 5) condition, whereas 49% of CCMN was released from CDSCM within the same time in a physiological pH 7.4 condition. The complete drug release was observed after 8 days of study in acidic pH 5, and it was observed that the CCMN presence in the CDSCM was about 36.8±2%, calculated using Equation 1. The higher release rate of CCMN in the acidic medium than in the basic medium is due to the acid-catalyzed hydrolysis of the ester linkage. 54,55 As a result, the rate of CCMN release in physiological pH is lower than in acidic

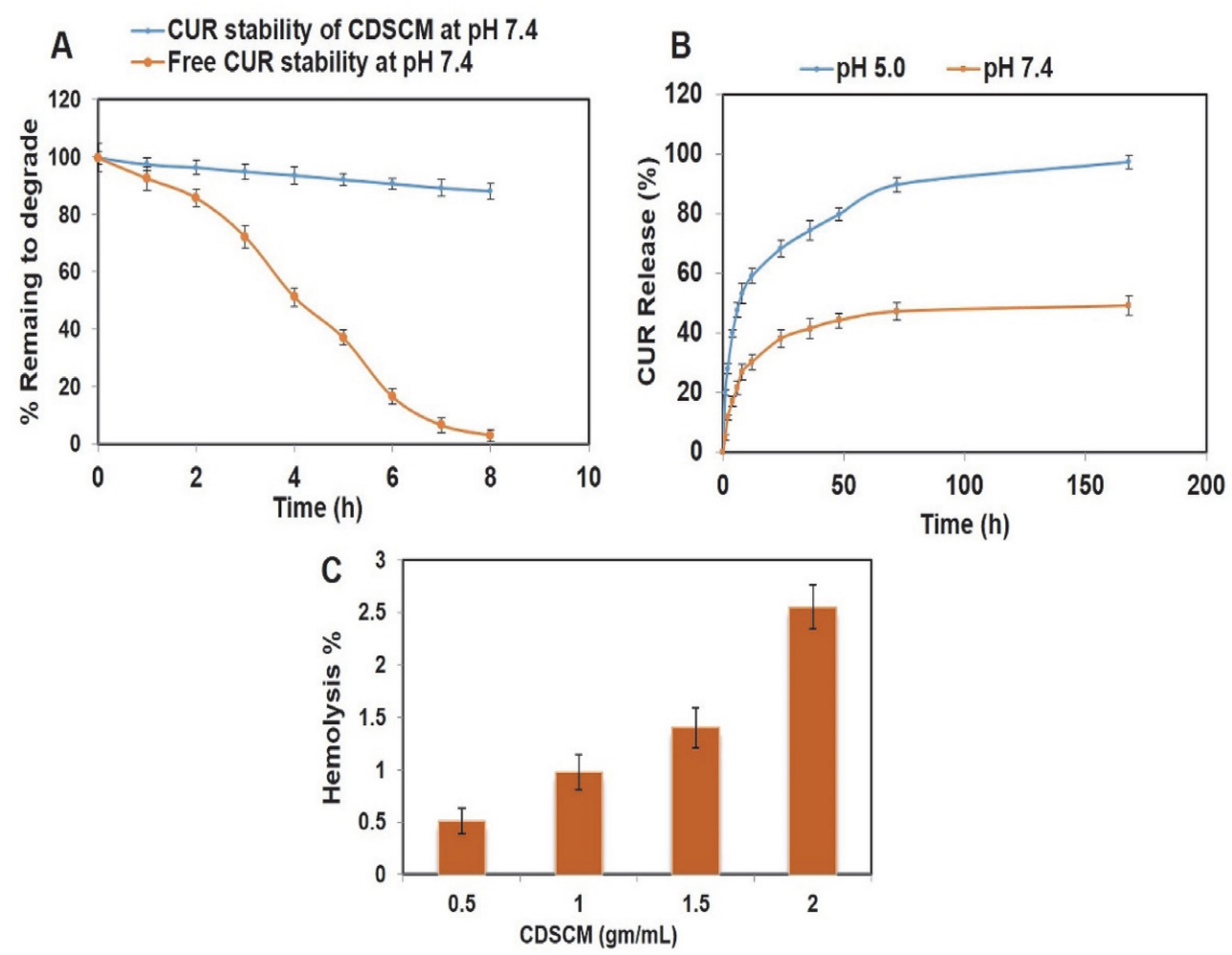


Figure 6: (a) Stability studies of CCMN and CDSCM, (b) Release profiles of CCMN from CDSCM under different conditions, and (c) Hemocompatibility assay of CDSCM

pH. Thus, CDSCM is applicable for sustained CCMN delivery and helps overcome first-pass metabolism. 56,57 The mechanism of drug release from CDSCM may depend on the release pattern in specific pH mediums. Release kinetic models were established for both acidic and basic medium, revealing that in the acidic medium, the release followed the first-order kinetic model, identified by its highest R2 value of 0.943 (Table 1). This indicates that the rate of drug release decreases exponentially over time as the drug concentration in the delivery system decreases. This release mechanism likely involves diffusion through a matrix or dissolution of the drug from a reservoir. The acidic pH may facilitate this diffusion by swelling the nanomicelles and breaking the ester bond, releasing CCMN into the medium. On the other hand, at pH 7.4, a basic medium, CCMN was released from the CDSCM following the Higuchi release kinetic model with the highest R2 value of 0.802 suggests the release of CCMN diffusion through polymeric matrix.

Table 1: The release kinetics from the CDSCM

pH of the medium	pH 5	pH 7.4			
	R ² Value				
Zero Ordar Model	0.5676	0.516			
1st Order model	0.9432	0.581			
korsmayar peppas model	0.5498	0.722			
Higuchi model	0.8371	0.802			
Hixson Crowell model	0.8313	0.559			

Hemocompatibility is an essential criterion for evaluating compatibility regarding hemoglobin release from RBC by drug-loaded nanoparticles for the safety and biocompatibility of nano-drug formulation. Drugs associated with nanoparticles can damage the RBC partially or fully.

A hemolytic study determined the percentage of hemoglobin released from RBC. After CDSCM and RBCs interact, hemoglobin from the damaged RBCs could be released. A UV-visible spectrophotometer measured the absorbance of hemoglobin³⁰, and was calculated in percentage. After sufficient time of incubation of CDSCMs with RBC, it was observed that around 2.5% of hemoglobin was released at the highest concentration of CDSCM (2mg/mL), as shown in **Figure 6c**. This signifies that our nano-formulation of CDSCM is compatible with RBC and blood, so these nano micelles are also applicable in intravenous administration.^{58–60}

After three days of diabetic induction, it was observed that most of the animals had FBG levels of 284 ± 9 mg/dL. Consider those animals as diabetic animals, and those with fasting blood glucose levels ≤ 145 mg/dL were not considered for the study. After the diabetic induction, a gradual body weight loss was observed (Figure 7C) in group II, but a slight increase in body weight in group III animals was observed. A significant increase in body weight of group-IV (CDSCM receiving group) was observed compared to group-V (diabetic control/standard drug) animals. The findings above highlight the significance of inducing diabetes about body weight and the possible contribution of CDSCM in addressing the alterations in body weight linked to diabetes.

The FBG level of overnight-fasted animals was measured every four days. A gradual increase in FBG level was observed (Figure 7A) in group II, but a gradual decrease in FBG level was observed in groups III, IV, and V. The non-diabetic control group I did not see any substantial alteration in fasting blood glucose (FBG) levels. The decrease in FBG level in users of CDSCM in group IV was substantially greater than in recipients of the conventional medicine in group V. The maximum decrease in blood glucose level was observed (Figure 7B) after 21 days of treatment in CDSCM recipients in group IV. The changes in

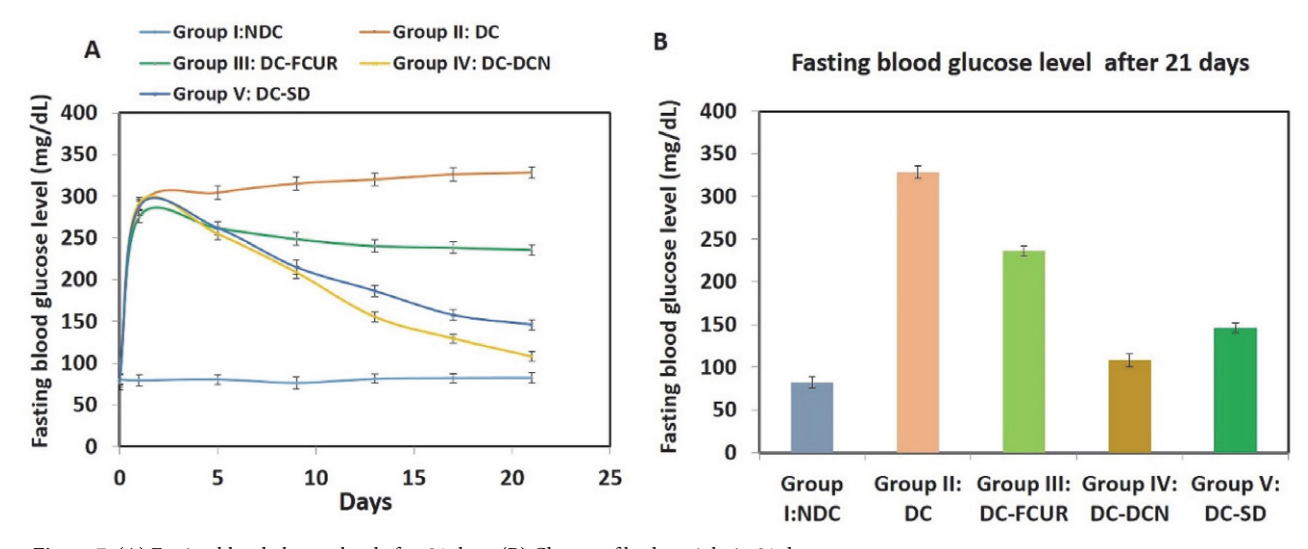


Figure 7: (A) Fasting blood glucose level after 21 days. (B) Change of body weight in 21 days.

Table 2. Biochemical parameters after 21 days of treatment

Parameter	Group I: NDC	Group II: DC	Group III: DC-FCUR	Group IV: DC-DCN	Group V: DC-SD
HbA1c (%)	5.70 ± 0.23	11.03 ± 0.31	8.55 ± 0.22	6.04 ± 0.20	6.89 ± 0.16
Serum creatinine (mg/dL)	0.81 ± 0.05	$1.51 \pm 0.04^{*}$	$1.11 \pm 0.03^*$	1.01 ± 0.04	1.17 ± 0.04
Serum uric acid (mg/dL)	$3.10 \pm 0.40^{**}$	$5.30 \pm 0.20^*$	$4.12 \pm 0.31^{**}$	$3.62 \pm 0.27^{*}$	4.51 ± 0.52
Serum cholesterol (mg/dL)	$83.0 \pm 1.1^{**}$	$157.1 \pm 1.7^{**}$	$109.0 \pm 1.2^{**}$	$91.1 \pm 0.9^*$	$124.0 \pm 2.1^*$
Serum triglycerides (mg/dL)	$90.0 \pm 1.2^*$	$156.3 \pm 1.9^{**}$	$121.7 \pm 2.2^{**}$	$95.0 \pm 1.4^*$	$111.0 \pm 3.1^{**}$
SGPT (IU/L)	70.0 ± 1.1	$170.6 \pm 3.8^{**}$	$92.6 \pm 3.1^{**}$	72.0 ± 1.0	80.1 ± 1.0
SGOT (IU/L)	$121.2 \pm 2.3^{**}$	$255.3 \pm 4.4^{**}$	$200.3 \pm 2.3^{**}$	$136.2 \pm 2.4^{**}$	$140.3 \pm 2.3^{**}$
HDL cholesterol (mg/dL)	$51.1 \pm 1.3^{**}$	$32.1 \pm 2.1^{**}$	$38.5 \pm 1.4^{**}$	$44.5 \pm 1.5^*$	$43.1 \pm 1.4^*$
LDL cholesterol (mg/dL)	$21.0 \pm 1.3^*$	$88.8 \pm 2.4^{**}$	$44.2 \pm 1.5^*$	$33.5 \pm 1.6^*$	$61.8 \pm 1.7^{**}$
ALP (IU/L)	$170.0 \pm 1.5^{**}$	$233.0 \pm 3.1^{**}$	$203.1 \pm 2.5^{**}$	$185.1 \pm 2.2^{**}$	$211.1 \pm 2.2^{**}$
Hexokinase (U/mL)	1.65 ± 0.11	0.25 ± 0.03	1.04 ± 0.12	1.47 ± 0.21	1.14 ± 0.32
G6PD (U/mL)	$22.6 \pm 1.4^{**}$	$85.4 \pm 2.1^{**}$	$62.6 \pm 2.5^{**}$	$29.0 \pm 2.8^{**}$	$38.8 \pm 1.8^*$
LDH (U/mL)	$13.6 \pm 0.7^*$	$26.8 \pm 1.4^{**}$	$20.8 \pm 0.8^*$	15.8 ± 0.8	17.7 ± 1.0

Data represent mean \pm S.D (n = 3). **p < 0.05; *p < 0.01.

FBG concentrations reflect the effect of interventions on glucose metabolism. The observed reduction in fasting blood glucose (FBG) levels across groups III, IV, and V provides evidence of the potential efficacy of these therapies in managing diabetes. The observed difference in the rate of reduction in fasting blood glucose (FBG) level between group IV (the group receiving the CDSCM treatment) and group V may be attributed to the unique mechanism of action of CDSCM. The faster rate of decrease in FBG levels in the CDSCM group (IV) compared to the conventional drug group (V) demonstrates the potential of CDSCM as a promising strategy for controlling glucose in diabetes management.

Biochemical parameters of all the experimental animals were measured on the 21st days after induction of diabetes and before induction of diabetes (Table 2), which shows that, the levels of HbA1c, serum creatinine, serum uric acid, serum cholesterol, serum triglycerides, SGPT, SGOT, HDL, LDL, ALP, Hexokinase, G6PD, and LDH have no unexpected changes in the non-diabetic control group I but significant increases (except for HDL and Hexokinase) in the group II. Mild increases were observed in the group III animals, and significant inverse phenomena were observed in groups IV and V. Hexokinase and HDL remarkably increased in CDSCM-receiving group IV compared to diabetic control group II and standard drug-receiving group V. The consistency of high FBG levels in the animal group indicates high glycated hemoglobin (HbA1c).61 After 21 days, the HbA1c levels of animals in group IV treated with CDSCM were lower. This decrease in HbA1c reflects the improved blood sugar management made possible by the administration of CDSCM. In addition, the investigation revealed a correlation between skeletal muscle mass and creatinine levels. As body weight decreased, creatinine levels increased, associated with an increased risk of type II diabetes.³⁷ Notably, animals treated with CDSCM had

significantly lower creatinine levels than those treated with free CCMN and the standard drug. This phenomenon suggests that CDSCM can potentially reduce the incidence of type II diabetes. The uric acid levels in the blood have emerged as valuable markers for various diseases, including stroke, hypertension, cardiac complications, and diabetes. 38,62 CDSCM also decreased serum uric acid levels, suggesting a potential improvement in the associated health risks. The investigation also explored diabetic dyslipidemia, a disorder characterized by abnormal lipid levels, including cholesterol, triglycerides, and distinct lipoprotein fractions. This condition is closely associated with type II diabetes. 38,63 Remarkably, animals treated with CDSCM exhibited fewer lipid abnormalities than the control group, indicating a potential function for CDSCM in diabetic dyslipidemia management.

The enzymatic focus of the investigation was on hexokinase, an enzyme with a negative correlation to diabetes. Notable was the increase in hexokinase levels in animals treated with CDSCM, which may have contributed to enhanced glucose metabolism. G6PD, an enzyme relevant to type II diabetes, is typically characterized by decreased tissue levels that contribute to increased blood levels due to metabolic alterations. Nonetheless, administration of CD-SCM decreased blood levels of G6PD, indicating a return to metabolic equilibrium. Type II diabetes includes a variety of metabolic disorders involving enzymes such as hexokinase, G6PD, LDH, SGPT, SGOT, and ALP, among others. 64,65 These enzymes exhibit altered concentrations in associated tissues and blood. The CDSCM treatment significantly decreased the blood levels of these enzymes compared to other treatments, according to the study's findings. Our studies amalgamate chemical synthesis and nanotechnology to increase bioavailability and deliver poorly water-soluble, highly degradable phytochemical curcumin in treating type II diabetes.

4. Discussion

In this study, the CHT-CCMN conjugate was synthesized successfully. The polymer prodrug molecule was then converted to the nano micelles form, a transformation that not only demonstrates the versatility of our research but also its potential for practical applications. The FTIR and NMR evaluation confirms that the polymer and the drug curcumin were chemically conjugated, proving our success. It was discovered that the conjugate was readily soluble in both an aqueous and an organic solvent, a characteristic that enhances its potential applications. After conjugation, the lipophilic compound CCMN and the hydrophilic polymer CHT form an amphiphilic conjugate, a unique feature that further enhances its potential. In an aqueous environment, the amphiphilic conjugate self-assembled into a micelle at a concentration of 0.4644 mg/mL, a finding that underscores its stability and accessibility. Due to the low CMC value, the nano micelles signify its stability, prolonging blood circulation and making it accessible for the drug's targeting. This feature in stills confidence in its potential for drug delivery systems.⁶⁶ The nano micelles exhibited an average hydrodynamic size range of 57 ± 6 nm, as measured by a zeta seizer. The majority of the particles were concentrated within a very limited range. The micelle's polydispersity index was found to be 0.19, which signifies the homogeneity of micelle size. From these, it is understood that micelles are not aggregated and create a proper dispersion in aqueous medium. The zeta potential of the micelle was -34.8 mV, which suggests that the micelles' surface are highly negatively charged, which could help them repel each other, accumulate into the aqueous medium, and provide better stability. These negative surface charges and smaller sizes may help micelles escape reticuloendothelial system internalization. 67,68 The SEM and TEM examination were conducted to morphologically characterize the CDSC micelles by microscopic inspection. The scanning electron microscope (SEM) picture revealed that the lyophilized powder of the CDSCM formed a nearly spherical and aggregated thin film. However, in order to get a precise comprehension, these micelles are examined using transmission electron microscopy (TEM), revealing their spherical shape and particle sizes ranging from around 50±10 nm. This provides the similarity with the hydrodynamic size of the prepared nano micelles. The morphological evaluation of the nano micelles provides a clear understanding of the size and shape of the nano micelles, which is acceptable for the in vivo characterization, and better homogeneous biodistribution will occur.⁶⁹

The degradation study found that at physiological pH 7.4, more than 90% of CDSCM remained to degrade within eight hours. In comparison, free CCMN degraded almost entirely under the same conditions. This contrast emphasizes the stability of CDSCM to maintain its structural strength in the physiological environment. Moreover, CDSCM showed a longer drug release duration at the

physiological pH compared to the medium's acidic pH level. This extended drug release profile presents the potential for achieving controlled drug delivery by assuring a constant drug release from micelles. In addition, CDSCM's ability to release drugs under acidic pH conditions enables its use in various medical conditions where drug release is required in acidic environments, thereby expanding its versatility in drug delivery systems. ^{70,71} The effect of fasting blood glucose (FBG) levels on animals treated with CDSCM was significantly greater than that of unbound CCMN and the standard drug glibenclamide.

Interestingly, the effects of CDSCM on body weight in diabetic-induced animals were found to be less severe than those of free CCMN and the conventional drug. The difference suggests that CDSCM may have a more targeted and potent effect on glucose regulation, potentially allowing for a more targeted method of treating elevated FBG levels. In addition, the consistent elevation of FBG levels in these animals suggests the presence of an elevated amount of glycated hemoglobin (HbA1c), highlighting the chronic nature of the diabetic condition under study.⁷² After 21 days, HbA1c levels were significantly reduced in animals treated with CDSCM, according to this research. This correlation can be explained by the direct relationship between skeletal muscle mass and creatinine levels, where creatinine levels progressively increase as body weight decreases, increasing the risk of type II diabetes.⁷³ Notably, the creatinine levels of CDSCM-treated animals were substantially lower than those of CCMN-free and standard-drug-treated animals. Notably, treatment with CD-SCM increased hexokinase enzyme levels, which may have improved glucose metabolism. Glucose-6-phosphate dehydrogenase (G6PD) is an additional enzyme associated with type II diabetes.

Nevertheless, administration of CDSCM reduced blood glucose-6-phosphate dehydrogenase (G6PD) levels, suggesting a restoration of metabolic equilibrium. Several metabolic disorders involving enzymes such as hexokinase, G6PD, LDH, SGPT, SGOT, and ALP, which exhibit altered concentrations in tissues and blood, are associated with Type II diabetes. Compared to other interventions, the CDSCM treatment substantially decreased blood enzyme levels. The above results could indicate that CDSCM restores the normal metabolic process in group IV more efficiently than in other diabetic groups. The effect of FBG on CDSCM capacity was significantly more than that of accessible CCMN and standard drug glibenclamide, and the impact on body weight of CDSCM-treated animals was less than that of free CCMN and standard drug-treated diabetic induced animals.

5. Conclusion

In this study, we have successfully synthesized a prodrug of chitosan-curcumin conjugate that self-assem-

bled in an aqueous environment as nano-micelles, where chitosan provided the hydrophilic outer backbone and curcumin the lipophilic core of the micelles. The chitosan di-succinyl curcumin micelles have curcumin in their backbone and entrap curcumin in their inner core, enhancing the solubility and stability of curcumin in many folds. Curcumin is sustainably released from micelles at physiological and acidic pH because there are ester bonds between chitosan and curcumin. The micelles play a pivotal role in declining the fasting blood glucose level and normalizing the related biochemical parameters of type II diabetic animals. The findings suggest that nano micelles have a notable effect in restoring the metabolic pathway that is disrupted in Type-II diabetes mellitus, as compared to both glibenclamide (the conventional treatment) and free curcumin. In future studies, these developments explore multidrug delivery in the form of conjugated prodrugs and entrapment in the micelle core. The amount of drug to be delivered can be increased as needed, prolonging the delivery time, and can be used for multiple other chronic biomedical conditions.

Author Contributions: Conceptualization: Sk Mosiur Rahaman and Ranu Biswas, Abimanyu Sugumaran.; Study execution, Data collection, Analysis, and interpretation of results: Sk Mosiur Rahaman, Ranu Biswas and Gouranga Dutta; Writing-original draft: Sk Mosiur Rahaman and Gouranga Dutta; Writing-review and editing: Sk Mosiur Rahaman, Ranu Biswas, Abimanyu Sugumaran, Mohamed M. Salem, Mounir M. Salem-Bekhit, Mohamed Abd El Rahman and Mohammed Gamal. Figures and Tables: Sk Mosiur Rahaman, Gouranga Dutta. All the authors have confirmed the manuscript for the submission proceedings.

Funding: The authors would like to extend their sincere appreciation to the Researchers Supporting Project Number (RSPD2024R986), King Saud University, Riyadh, Saudi Arabia.

Institutional Review Board Statement: The Institutional Animal Ethics Committee of Jadavpur University, Kolkata, India (JU/IAEC-22/30) approved the animal study protocol.

Data Availability Statement: Current study data are available from the corresponding author upon reasonable request

Acknowledgments: The authors are thankful to Head, Department of Pharmaceutical Technology, Jadavpur University, Kolkata, West Bengal, India.

Conflicts of Interest: The author declares that there is no financial or personal conflict of interest associated with the work reported in this paper.

6. Reference

- 1. QX. Zhang, E. Kupczyk, P. Schmitt-Kopplin, C. Mueller, *Drug Discov. Today.* **2022**, *27*, 103331.
 - DOI:10.1016/j.drudis.2022.07.016
- S. Park, H. Lee, W. Cho, H. G. Woo, H. Lim, S. Kim, S. Y. Rhee, D. K. Yon, *Obes. Rev.* 2024, 25, e13714.
 DOI:10.1111/obr.13714
- N. Esser, S. Legrand-Poels, J. Piette, A. J. Scheen, N. Paquot, Diabetes Res. Clin. Pract. 2014, 105, 141–150.
 DOI:10.1016/j.diabres.2014.04.006
- 4. D. A. Domingo-Lopez, G. Lattanzi, L. H. J. Schreiber, E. J. Wallace, R. Wylie, J. O'Sullivan, E. B. Dolan, G. P. Duffy, *Adv. Drug Deliv. Rev.* **2022**, *185*, 114280. **DOI**:10.1016/j.addr.2022.114280
- L. A. DiMeglio, C. Evans-Molina, R. A. Oram, *Lancet.* 2018, 391, 2449–2462. DOI:10.1016/S0140-6736(18)31320-5
- 6. S. E. Kahn, *Diabetologia*. **2003**, *46*, 3–19. **DOI**:10.1007/s00125-002-1009-0
- Y. Li, W. Zhang, R. Zhao, X. Zhang, Bioact. Mater. 2022, 15, 392–408. DOI:10.1016/j.bioactmat.2022.02.025
- 8. W. Lu, F. Khatibi Shahidi, K. Khorsandi, R. Hosseinzadeh, A. Gul, V. Balick, *J. Food Biochem.* **2022**, *46*, e14358. **DOI**:10.1111/jfbc.14358
- B. Salehi, Z. Stojanović-Radić, J. Matejić, M. Sharifi-Rad, N. V. Anil Kumar, N. Martins, J. Sharifi-Rad, *Eur. J. Med. Chem.* 2019, 163, 527–545. DOI:10.1016/j.ejmech.2018.12.016
- A. Sugumaran, J. Sadhasivam, P. Gawas, V. Nutalapati, R. Pandian, S. Kumar Perumal, *Mater. Sci. Eng. B.* 2022, 286, 116047. DOI:10.1016/j.mseb.2022.116047
- S. Fuloria, J. Mehta, A. Chandel, M. Sekar, N. N. I. M. Rani, M. Y. Begum, V. Subramaniyan, K. Chidambaram, L. Thangavelu, R. Nordin, et al., Front. Pharmacol. 2022, 13, 820806.
 DOI:10.3389/fphar.2022.820806
- N. Agrawal, M. Jaiswal, Eur. J. Med. Chem. Reports. 2022, 6, 100081. DOI:10.1016/j.ejmcr.2022.100081
- V. Ruiz de Porras, L. Layos, E. Martínez-Balibrea, *Semin. Cancer Biol.* **2021**, *73*, 321–330.
 DOI:10.1016/j.semcancer.2020.09.004
- Y. Zhong, C. Liu, J. Feng, J. Li, Z. Fan, Exp. Ther. Med. 2020, 20, 1856–1870. DOI:10.3892/etm.2020.8915
- S. K. Jain, J. Rains, J. Croad, B. Larson, K. Jones, *Antioxid. Redox Signal.* 2009, 11, 241–249. DOI:10.1089/ars.2008.2140
- O. Bozkurt, B. Kocaadam-Bozkurt, H. Yildiran, Food Funct.
 2022, 13, 11999–12010. DOI:10.1039/D2FO02625B
- F. Pivari, A. Mingione, C. Brasacchio, L. Soldati, *Nutrients*, 2019, 11, 1837. DOI:10.3390/nu11081837
- S. Ibrahim, T. Tagami, T. Kishi, T. Ozeki, *Int. J. Pharm.* 2018, 540, 40–49. DOI:10.1016/j.ijpharm.2018.01.051
- H. Ringsdorf, *J. Polym. Sci. Polym. Symp.* 1975, 51, 135–153.
 DOI:10.1002/polc.5070510111
- A. Anand, B. R. Iyer, C. Ponnusamy, R. Pandiyan, A. Sugumaran, *Cardiovasc. Hematol. Agents Med. Chem.* 2020, 18, 45–54. DOI:10.2174/1871525718666200203112502
- 21. I. Aranaz, A. R. Alcántara, M. C. Civera, C. Arias, B. Elorza, A. Heras Caballero, N. Acosta, *Polymers (Basel).* **2021**, *13*,

- 3256. **DOI:**10.3390/polym13193256
- J. Sharifi-Rad, C. Quispe, M. Butnariu, L. S. Rotariu, O. Sytar, S. Sestito, S. Rapposelli, M. Akram, M. Iqbal, A. Krishna, et al., *Cancer Cell Int.* 2021, 21, 318.
 DOI:10.1186/s12935-021-02025-4
- D. Ghosh Dastidar, S. Saha, G. Dutta, S. Abat, N. Guha, D. Ghosh, *Mater. Res. Express.* 2020, 7, 015031.
 DOI:10.1088/2053-1591/ab637f
- 24. A. Sugumaran, V. Mathialagan, *Curr. Pharm. Des.* **2020**, *26*, 5174–5187. **DOI**:10.2174/1381612826666200625110950
- V. Krishnaswami, A. Sugumaran, V. Perumal, M. Manavalan,
 D. P. Kondeti, S. K. Basha, M. A. Ahmed, M. Kumar, S. Vija-yaraghavalu, *Curr. Drug Targets.* 2022, 23, 1330–1344.
 DOI:10.2174/1389450123666220822094248
- S. Jain, R. Jain, M. Das, A. K. Agrawal, K. Thanki, V. Kushwah, RSC Adv. 2014, 4, 29193–29201. DOI:10.1039/ C4RA04237A
- M. Li, M. Gao, Y. Fu, C. Chen, X. Meng, A. Fan, D. Kong,
 Z. Wang, Y. Zhao, *Colloids Surf. B Biointerfaces.* 2016, 140,
 11–18. DOI:10.1016/j.colsurfb.2015.12.025
- R. Raveendran, C. K. S. Pillai, G. S. Bhuvaneshwar, C. P. Sharma, J. Nanopharmaceutics Drug Deliv. 2014, 2, 36–51.
 DOI:10.1166/jnd.2014.1046
- 29. S. Dey, K. Sreenivasan, *Carbohydr. Polym.* **2014**, *99*, 499–507. **DOI:**10.1016/j.carbpol.2013.08.067
- Sauraj, S. U. Kumar, P. Gopinath, Y. S. Negi, *Carbohydr. Polym.* 2017, 157, 1442–1450. DOI:10.1016/j.carbpol.2016.09.096
- S. V. Lale, A. Kumar, S. Prasad, A. C. Bharti, V. Koul, *Biomacromolecules*. 2015, *16*, 1736–1752.
 DOI:10.1021/acs.biomac.5b00244
- C. Ponnusamy, A. Sugumaran, V. Krishnaswami, R. Kandasamy, S. Natesan, *IET Nanobiotechnol.* 2019, *13*, 868–874.
 DOI:10.1049/iet-nbt.2019.0130
- F. Shafiee, E. Khoshvishkaie, A. Davoodi, A. Dashti Kalantar,
 H. Bakhshi Jouybari, R. Ataee, *Medicines*. 2018, 5.
 DOI:10.3390/medicines5010001
- 34. M. Wahab, A. Bhatti, P. John, *Polymers (Basel)*. **2022**, *14*, 3138. **DOI**:10.3390/polym14153138
- 35. P. L. Cruz, I. C. Moraes-Silva, A. A. Ribeiro, J. F. Machi, M. D. T. de Melo, F. dos Santos, M. B. da Silva, C. M. C. Strunz, E. G. Caldini, M.-C. Irigoyen, *BMC Endocr. Disord.* **2021**, *21*, 133. **DOI:**10.1186/s12902-021-00795-6
- P. Rathore, A. Mahor, S. Jain, A. Haque, P. Kesharwani, RSC Adv. 2020, 10, 43629–43639. DOI:10.1039/D0RA07640F
- 37. G. Chandirasegaran, C. Elanchezhiyan, K. Ghosh, *Biomed. Pharmacother.* **2018**, 99, 227–236. **DOI:**10.1016/j.biopha.2018.01.007
- M. U. Akbar, K. M. Zia, M. S. H. Akash, A. Nazir, M. Zuber, M. Ibrahim, *Int. J. Biol. Macromol.* 2018, 120, 2418–2430.
 DOI:10.1016/j.ijbiomac.2018.09.010
- Y. M. El-Far, M. M. Zakaria, M. M. Gabr, A. M. El Gayar, L. A. Eissa, I. M. El-Sherbiny, *Nanomed.* 2017, *12*, 1689–1711.
 DOI:10.2217/nnm-2017-0106
- 40. M. F. Elsadek, B. M. Ahmed, *Saudi J. Biol. Sci.* **2022**, *29*, 1402–1406. **DOI:**10.1016/j.sjbs.2021.11.035
- 41. S. Manandhar, E. Sjöholm, J. Bobacka, J. M. Rosenholm, K. K.

- Bansal, *J. Nanotheranostics.* **2021**, *2*, 63–81. **DOI:**10.3390/jnt2010005
- 42. J. Pan, K. Rostamizadeh, N. Filipczak, V. Torchilin, *Molecules*. **2019**, *24*, 1035. **DOI:**10.3390/molecules24061035
- Sauraj, S. U. Kumar, V. Kumar, R. Priyadarshi, P. Gopinath, Y.
 Negi, *Carbohydr. Polym.* 2018, 188, 252–259.
 DOI:10.1016/j.carbpol.2018.02.006
- 44. J. Wang, J.-Z. Jiang, W. Chen, Z.-W. Bai, *Carbohydr. Polym.* **2016**, *145*, 78–85. **DOI**:10.1016/j.carbpol.2016.03.022
- A. Praveen, D. Prasad, S. Mishra, S. Nagarajan, S. R. Chaudhari, *Food Chem.* 2021, *341*, 128646.
 DOI:10.1016/i.foodchem.2020.128646
- B. N. Waghela, A. Sharma, S. Dhumale, S. M. Pandey, C. Pathak, *PLoS One.* 2015, *10*, e0117526.
 DOI:10.1371/journal.pone.0117526
- 47. N. M. L. Hansen, D. Plackett, *Polym. Chem.* **2011**, *2*, 2010–2020. **DOI:**10.1039/c1py00086a
- M. Huo, Y. Zhang, J. Zhou, A. Zou, D. Yu, Y. Wu, J. Li, H. Li, *Int. J. Pharm.* 2010, 394, 162–173.
 DOI:10.1016/j.ijpharm.2010.05.001
- P. R. Sarika, N. R. James, P. R. A. Kumar, D. K. Raj, T. V. Kumary, *Carbohydr. Polym.* 2015, *134*, 167–174.
 DOI:10.1016/j.carbpol.2015.07.068
- A. Sahu, U. Bora, N. Kasoju, P. Goswami, *Acta Biomater*.
 2008, 4, 1752–1761. DOI:10.1016/j.actbio.2008.04.021
- 51. H. Li, D. Hu, F. Liang, X. Huang, Q. Zhu, R. Soc. Open Sci. **2020**, 7, 192092. **DOI:**10.1098/rsos.192092
- 52. X. Zhang, Y. Huang, S. Li, *Ther. Deliv.* **2014**, *5*, 53–68. **DOI:**10.4155/tde.13.135
- 53. Y. Liu, K. Liu, C. Li, L. Wang, J. Liu, J. He, J. Lei, X. Liu, *RSC Adv.* **2017**, *7*, 36256–36268. **DOI:**10.1039/C7RA05913B
- L. Hu, P. Zhang, X. Wang, X. Cheng, J. Qin, R. Tang, *Carbohydr. Polym.* 2017, *178*, 166–179.
 DOI:10.1016/j.carbpol.2017.09.004
- L. Nicolle, C. M. A. Journot, S. Gerber-Lemaire, *Polymers (Basel)*. 2021, *13*, 4118. DOI:10.3390/polym13234118
- J. J. Milligan, S. Saha, Cancers (Basel). 2022, 14, 1741.
 DOI:10.3390/cancers14071741
- M. Ghezzi, S. Pescina, C. Padula, P. Santi, E. Del Favero, L. Cantù, S. Nicoli, *J. Control. Release.* 2021, 332, 312–336.
 DOI:10.1016/j.jconrel.2021.02.031
- 58. M. Rai, R. Pandit, S. Gaikwad, A. Yadav, A. Gade, *Nanotechnol. Rev.* **2015**, *4*, 161–172. **DOI:**10.1515/hsz-2015-0001
- N. Ghalandarlaki, A. M. Alizadeh, S. Ashkani-Esfahani, Biomed Res. Int. 2014, 2014, 1–23. DOI:10.1155/2014/394264
- Z. Li, M. Shi, N. Li, R. Xu, Front. Chem. 2020, 8, 589957.
 DOI:10.3389/fchem.2020.589957
- G. Chao, Y. Zhu, L. Chen, J. Diabetes Res. 2021, 2021.
 DOI:10.1155/2021/6626587
- 62. Q. Xiong, J. Liu, Y. Xu, *Int. J. Endocrinol.* **2019**, *2019*, 1–8. **DOI:**10.1155/2019/9691345
- 63. T. Hirano, *J. Atheroscler. Thromb.* **2018**, *25*, 771–782. **DOI:**10.5551/jat.RV17023
- M. Taher, T. M. F. S. Tg Zakaria, D. Susanti, Z. A. Zakaria, *BMC Complement. Altern. Med.* 2016, 16, 135.
 DOI:10.1186/s12906-016-1118-9

- S. K. Choudhary, G. Chhabra, D. Sharma, A. Vashishta, S. Ohri, A. Dixit, Evidence-Based Complement. Altern. Med. 2012, 2012, 1–10. DOI:10.1155/2012/293650
- G. Ottaviani, S. Wendelspiess, R. Alvarez-Sánchez, Mol. Pharm. 2015, 12, 1171–1179. DOI:10.1021/mp5006992
- K. Xiao, Y. Li, J. Luo, J. S. Lee, W. Xiao, A. M. Gonik, R. G. Agarwal, K. S. Lam, *Biomater.* 2011, 32, 3435–3446.
 DOI:10.1016/j.biomaterials.2011.01.021
- M. Zhang, S. Gao, D. Yang, Y. Fang, X. Lin, X. Jin, Y. Liu, X. Liu, K. Su, K. Shi, *Acta Pharm. Sin. B.* 2021, *11*, 2265–2285.
 DOI:10.1016/j.apsb.2021.03.033
- J. M. Caster, S. K. Yu, A. N. Patel, N. J. Newman, Z. J. Lee, S. B. Warner, K. T. Wagner, K. C. Roche, X. Tian, Y. Min, et al., Nanomed. :Nanotechnol. Biol. Med. 2017, 13, 1673–1683. DOI:10.1016/j.nano.2017.03.002

- Z. Yu, L. Ma, S. Ye, G. Li, M. Zhang, Carbohydr. Polym. 2020, 236, 115972. DOI:10.1016/j.carbpol.2020.115972
- N. A. Nasab, H. H. Kumleh, M. Beygzadeh, S. Teimourian, M. Kazemzad, *Artif. Cells Nanomed. Biotechnol.* 2018, 46, 75–81.
 DOI:10.1080/21691401.2017.1290648
- S. I. Sherwani, H. A. Khan, A. Ekhzaimy, A. Masood, M. K. Sakharkar, *Biomark. Insights* 2016, 11, 95–104.
 DOI:10.4137/BMI.S38440
- N. Harita, T. Hayashi, K. K. Sata, Y. Nakamura, T. Yoneda, G. Endo, H. Kambe, *Diabetes Care.* 2009, 32, 424–426.
 DOI:10.2337/dc08-1265

Povzetek

Sladkorna bolezen je kronična presnovna motnja, za katero je značilna povišana raven sladkorja v krvi, ki povzroča motnje v delovanju organov. Kurkumin, pridobljen iz kurkume, kaže obetavne lastnosti pri zdravljenju sladkorne bolezni tipa II. Amfipatska polimerna predzdravila so sintetizirali s konjugiranjem kurkumina s hitosanom prek sukcinil anhidrida. Nanomiceli, ki so nastali z dializo amfipatskega polimernega predzdravila, so bili sferični s povprečno hidrodinamsko velikostjo 57 nm. Študije sproščanja *in vitro* so pokazale 97-odstotno sproščanje kurkumina pri pH 5 v 7 dneh. V 21-dnevnem poskusu na diabetičnih miših so primerjali vpliv nanomicel, standardnih zdravil in prostega kurkumina na glukozo v krvi na tešče. Študija je pokazala postopno in nadzorovano sproščanje kurkumina iz nanomicel, kar kaže na njihov potencial pri zdravljenju sladkorne bolezni tipa II.



Except when otherwise noted, articles in this journal are published under the terms and conditions of the Creative Commons Attribution 4.0 International License